

## Electronic Supplementary Information (ESI)

### **Rapidly-Switchable Water-Sensitive Shape-Memory Cellulose/Elastomer Nano-composites**

By *Yong Zhu, Jinlian Hu\**, *Hongsheng Luo, Robert J Young, Libo Deng,*  
*Sheng Zhang, Ying Fan* and *Guangdou Ye*

Prof. J. L. Hu, Dr. Y. Zhu, and H. S. Luo  
Institute of Textiles and Clothing, Hong Kong Polytechnic University, Hung Hom  
Hong Kong

Prof. R. J. Young, and Dr. L. B. Deng  
Materials Science Centre, School of Materials, The University of Manchester, Oxford  
Road, Manchester, M13 9PL, UK

Prof. G. D. Ye, Dr. S. Zhang and Y. Fan  
State Key Laboratory of Polymer Materials Engineering (Sichuan University),  
Chengdu, 610065, China

\*To whom correspondence should be addressed. E-mail:  
tchujl@inet.polyu.edu.hk

This supplement includes:

Figure S1. SEM images of cryogenic fracture surface of CNW/TPUs after freezing in liquid nitrogen. (Gauge length=2 micron)

Figure S2. Demonstration of switchable water sensitive shape memory behavior of CNW/TPUs (TPUC30) at ambient condition (23 °C and 65% RH).

Figure S3. Dynamic mechanical analysis during heat sweep at 5 °C/min from -120 to 260 °C

The mathematical expression of percolation and Halpin-Kardos model

Figure S4. Evolution of FTIR spectrum of CNW/TPUs (TPUC20) during wetting and drying procedures

The description about the effectiveness of wetting and drying in CNW/TPUs by FTIR

Figure S5. FTIR analysis on the effect of water immersion time on the absorption of

carbonyl group in TPUC20 and TPU. (a) C=O stretching region of TPUC20; (b) C=O stretching region of TPU; (c) Peak position of free hydrogen bonded C=O stretching band for different water immersion time (~712 hour).

Figure S6. Weight ratio of absorbed water in CNW/TPUs during immersion in water. Dots represent the average values (number of individual measurement is 3)  $\pm$  standard deviation.

Figure S7. Polarized Raman spectra of the sample TPUC30 before deformation and after drying in deformed status respectively

References

Movie S1 provided as separate file.

### **S1. SEM of CNW/TPUs**

A JEOL JSM-6490 SEM instrument was used to investigate the morphology of the fracture surface of CNW/TPU film samples after freezing in liquid nitrogen. The surface observed was coated with gold on JEOL JFC-1100E ion sputter coater in advance. The SEM micrographs were obtained by using 7kV secondary electrons.

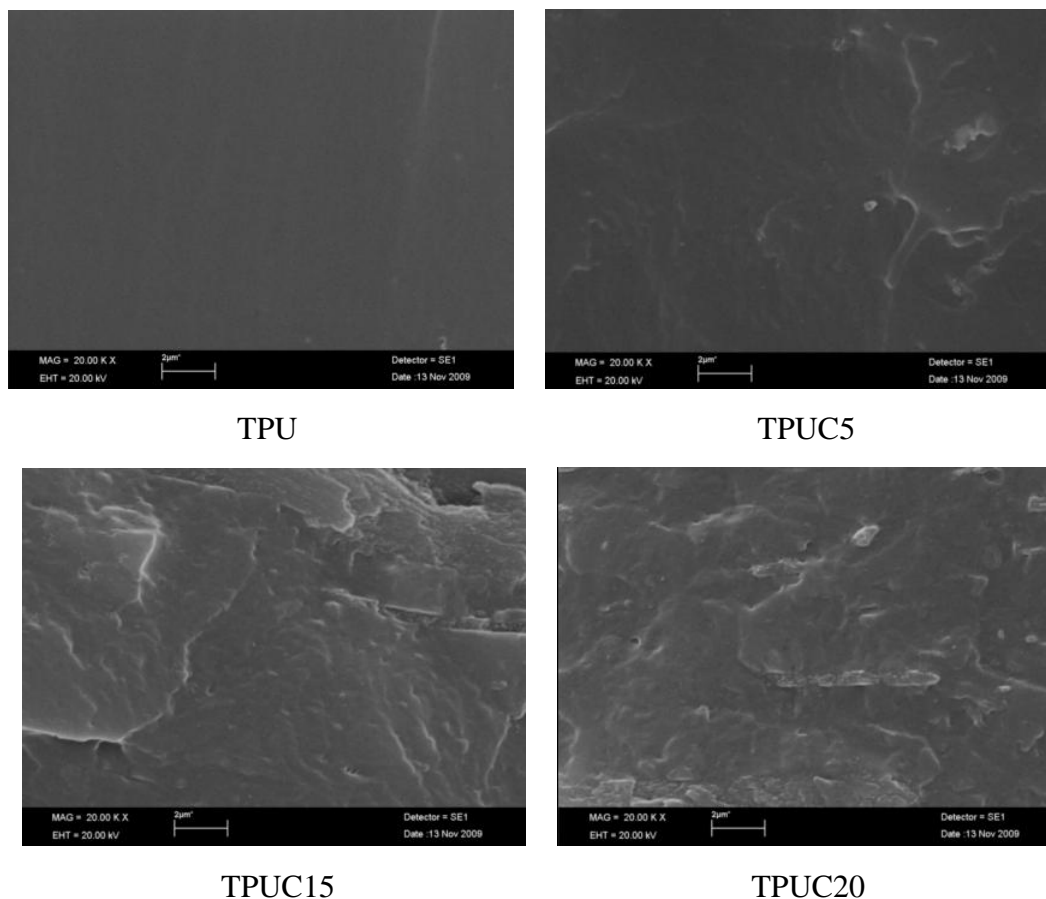


**Figure S1.** SEM images of cryogenic fracture surface of CNW/TPUs after freezing in liquid nitrogen. (Gauge length=2 micron)

## S2. Shape memory behavior of CNW/TPUs

The visualization of the rapidly-switchable shape memory behavior in CNW/TPU (TPUC30) is recorded in photographs shown in **Figure S2**, in which the wetting-drying programming is quite similar to those used in cyclic tensile test. This sample tape has been pre-stretched to 10.8cm from 2.3cm. Then the new original length recovered through water immersion is 3.7cm used for following stretching experiment and calculation. The stretching to a large elongation ( $\epsilon_m=191.9\%$ , length=10.8cm) is conducted. Then, upon dropping water onto the sample tape, the fixed strain ( $\epsilon_u=164.9\%$ , length=9.8cm) can quickly recover to the permanent shape

( $\epsilon_p$ (irreversible strain)=45.9%, length=5.4cm). As shown in Figure S2, the sharp recovery is completed mostly within 2 mins. The corresponding  $R_f$  and  $R_r$  calculated from the above results are 85.9 and 76.1% respectively. These results are somewhat deviated from the cyclic tensile test, in which  $R_f$  and  $R_r$  are 94.74% and 94.93% respectively in the 2st-3rd cycle of the cyclic tensile test ( $\epsilon_m = 100\%$ ) for TPUC30 (**Figure 3(b)**). The deviation is caused by the difference of stretching procedure and stretching extent. Also the water sensitive recovery is triggered by dropping water on a plate surface with a glass cover. It may be one of causes for the differential results. Besides, the moisture from ambient circumstance (23 °C and 65% RH) may give rise to a little of recovery during unloading. Notwithstanding, the rapid shape recovery behavior is visualized significantly.

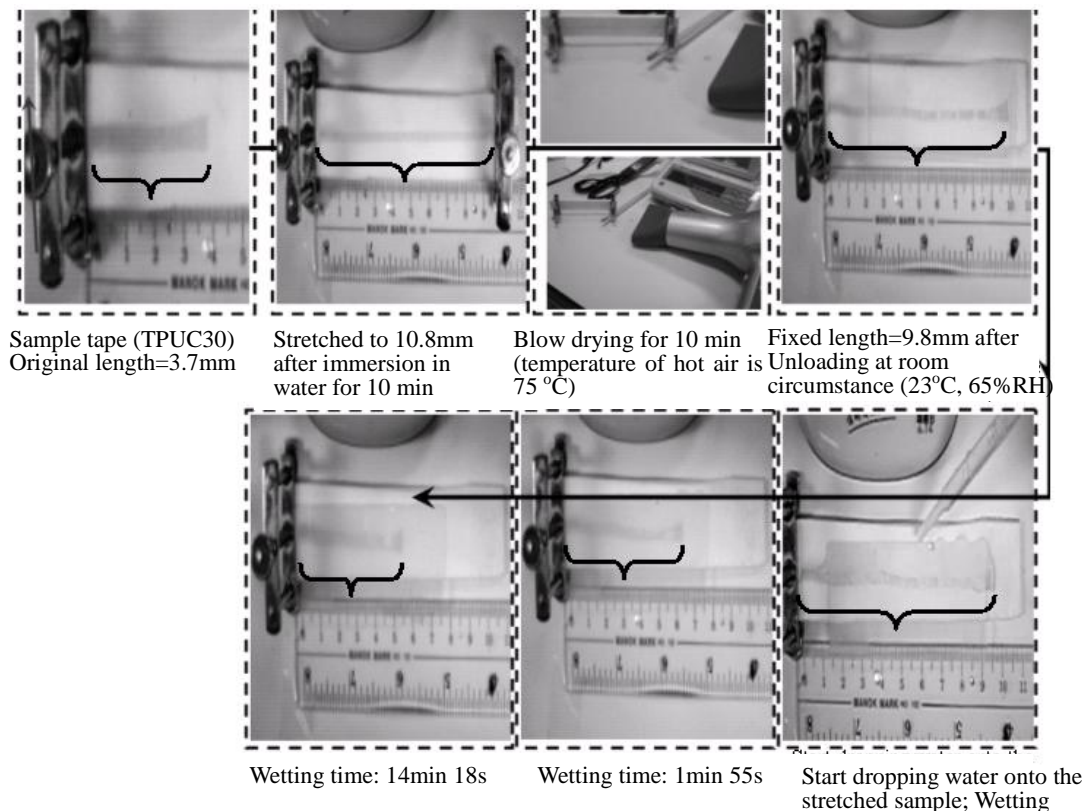


**Figure S2.** Demonstration of switchable water sensitive shape memory behavior of CNW/TPUs (TPUC30) at ambient condition (23 °C and 65% RH).

### S3. DMA of CNW/TPUs

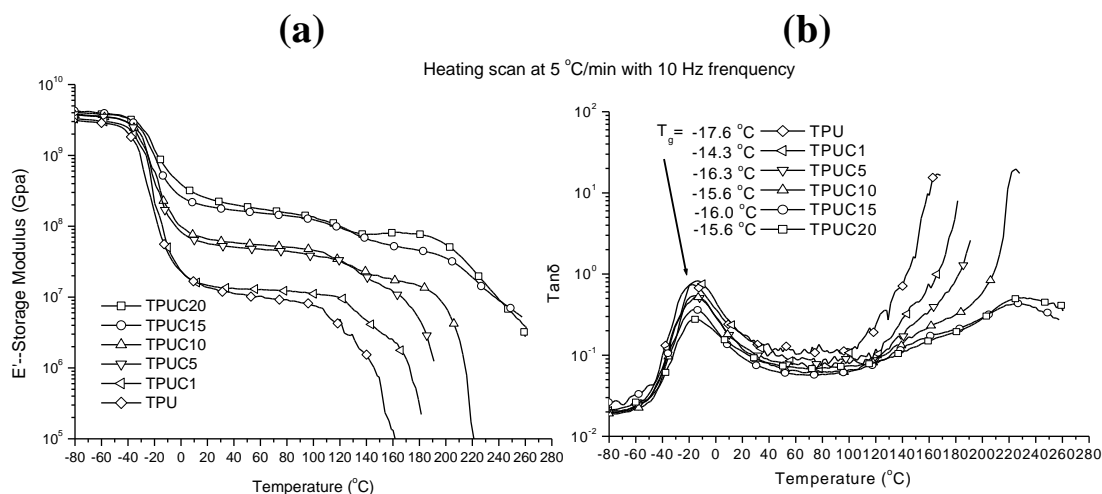


**Figure S3.** Dynamic mechanical analysis during heat sweep at 5 °C/min from -120 to 260 °C

#### The mathematical expression of percolation and Halpin-Kardos model

The mathematical expression of percolation model is reported previously<sup>1</sup> and shown below:

$$E' = \frac{(1 - 2\Psi + \Psi X_r) E'_s E'_r + (1 - X_r) \Psi E_r'^2}{(1 - X_r) E'_r + (X_r - \Psi) E'_s} \quad (1)$$

with

$$\Psi_r = X_r \left( \frac{X_r - X_c}{1 - X_c} \right)^{0.4}$$

where  $\psi$  is the percolation volume fraction of nano whiskers that participate in the load transfer;  $E'_s$  and  $E'_r$  are modulus of soft and rigid phase respectively;  $X_r$  is the volume fraction of rigid phase; the percolation volume fraction  $\psi$  is defined as the volume fraction of an “infinite” cluster of whiskers corresponding to the fraction of whiskers active in the load transfer from on whisker to another;  $X_r \geq X_c$  and  $X_c \geq 0.7/A$

(A is the aspect ratio of the nano whiskers) are the critical nano whisker volume fraction for the percolation network<sup>2</sup>.

In Halpin-Kardos model, the modulus of the individual piles in longitudinal and transverse directions can be derived from Halpin Tsai equations<sup>3</sup>. The longitudinal Young's modulus is given by:

$$E'_L = \frac{E'_s (1 + 2A\eta_L\phi_r)}{1 - \eta_L\phi_r} \quad (2)$$

The Young's modulus in transverse direction becomes:

$$E'_T = \frac{E'_s (1 + 2A\eta_T\phi_r)}{1 - \eta_T\phi_r} \quad (3)$$

$$\text{where } \eta_L = \frac{\frac{E_{tr}}{E_s} - 1}{\frac{E_{tr}}{E_s} + 2A} \quad \text{and} \quad \eta_T = \frac{\frac{E_{tr}}{E_s} - 1}{\frac{E_{tr}}{E_s} + 2}$$

The tensile storage modulus of the nano-composite can be derived from:

$$E' = \frac{4U_5(U_1 - U_5)}{U_1} \quad (4)$$

$$\text{with } U_1 = \frac{3Q_{11} + 3Q_{22} + 2Q_{12} + 4Q_{66}}{8}$$

$$U_5 = \frac{Q_{11} + Q_{22} - 2Q_{12} + 4Q_{66}}{8}$$

$$Q_{11} = \frac{E'_L}{(1 - \nu_{12}\nu_{21})}$$

$$Q_{22} = \frac{E'_T}{(1 - \nu_{12}\nu_{21})}$$

$$Q_{12} = \nu_{12}Q_{22} = \nu_{21}Q_{11}$$

$$Q_{66} = G'_{12}$$

where  $\nu_{12} = \phi_r \nu_r + \phi_s \nu_s$ ;  $G'_{12} = \frac{G'_s (1 + \eta \phi_r)}{1 - \eta \phi_r}$ ;  $\eta = \frac{G'_r / G'_s - 1}{G'_r / G'_s + 1}$  and  $\nu$  is the

Poisson's ratio defined as 0.3;  $G'$  is the shear modulus;  $\phi_r$  and  $\phi_s$  are the volume fraction of rigid and soft phase respectively.

**Figure 5** shows the fit curve in solid line based on percolation model, in which the parameters can be obtained from the experiments ( $E'_s$  (13.12 MPa) of DMA results and previous literature ( $E'_r=4\text{GPa}^4$ );  $X_c$  is equal to 4.76 vol% (0.7/A);  $E'_r$  refer to the neat whisker film<sup>5</sup>). The fit curve of dot line is from Halpin-Kardos model, in which A is 14.7 calculated from TEM images of whiskers;  $E'_s$  is 13.12 MPa from DMA results;  $E'_{tr}=5\text{GPa}^3$ ;  $E'_{lr}=105\text{GPa}^4$ ;  $\nu_s=0.3$ ,  $\nu_r=0.5$  and  $G'_r=1.77\text{GPa}^3$ ;

$$G'_s = \frac{E'_s}{2(1 + \nu_s)} = 4.4\text{MPa}.$$

#### S4. FTIR analysis

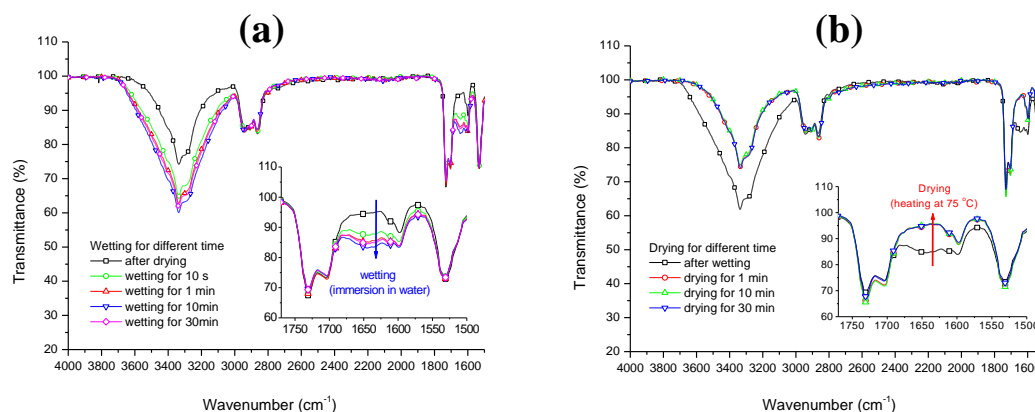


**Figure S4.** Evolution of FTIR spectrum for (a): wetting for different time and (b): drying for different time referred to TPUC20

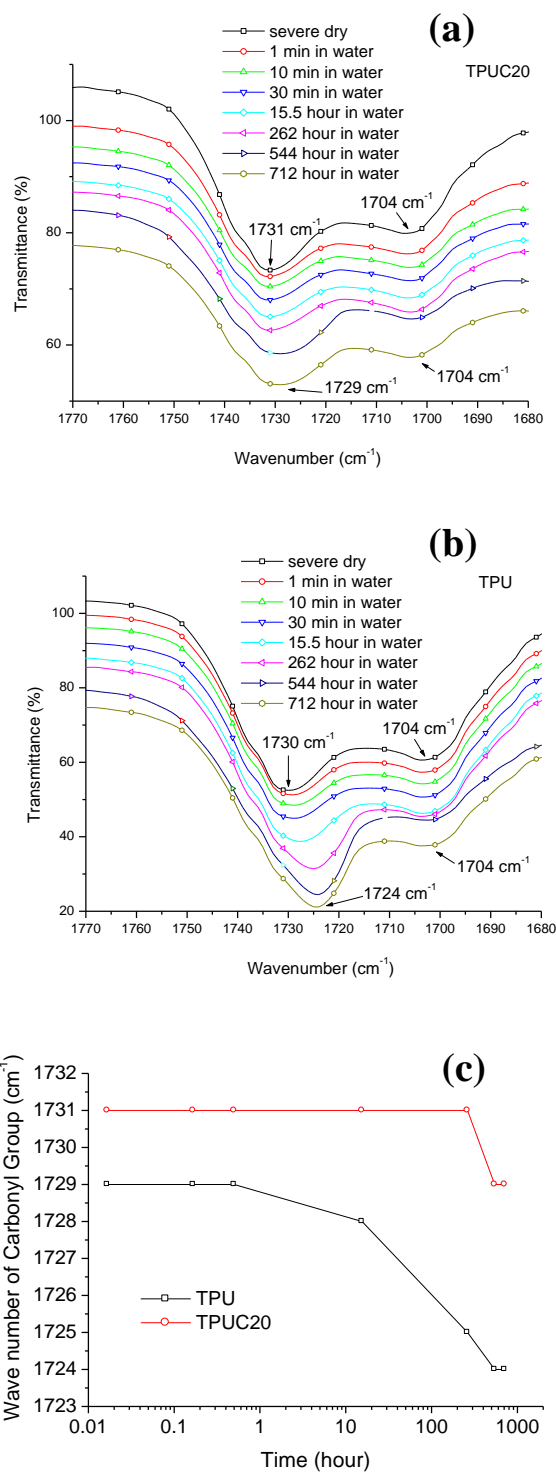


**Figure S5.** FTIR analysis on the effect of water immersion time on the absorption of carbonyl group in TPUC20 and TPU. (a) C=O stretching region of TPUC20; (b) C=O stretching region of TPU; (c) Peak position of free hydrogen bonded C=O stretching band for different water immersion time (~712 hour).

To confirm the effectiveness of the above drying and wetting, the FTIR spectrum of the sample (TPUC20) after wetting and drying for different time were traced. The results shown in **Figure S4** illustrated that the peak area at  $1641\text{ cm}^{-1}$  was increased (by wetting) or decreased (by drying) to a stable value even after wetting or drying for 1 min. Because ATR mode of FTIR is only used to detect the IR absorbance of the sample with several micros (0.5~5 micros) depth beyond the crystal surface into the sample, the FTIR absorbance response during drying-wetting cycles is much faster than  $E'$  variation by DMA. The cause should be that the water molecules of absorption and desorption during wetting or drying take more time to effect in whole bulk of CNW/TPUs. Therefore,  $E'$  from DMA shown in Figure 4 takes more time (about 10 min) to attain the switchable variation under alternate drying and wetting condition. It is also the base for the following switchable shape memory programming design.

It's worth noting that Huang et. al.<sup>6</sup> reported that in a commercial shape memory polyurethane immersed in water, the loosely bond water directly weakens the hydrogen bonding, and some water molecules form new double hydrogen bonds with two already hydrogen bonded C=O groups, and then lower the  $T_g$  to realize water driven shape recovery. Thereof, the infrared band of free C=O stretching at  $1724\text{ cm}^{-1}$  is observed to shift to the bonded one on at  $1701\text{ cm}^{-1}$  in the first 48 hour immersion. Such a shift of C=O stretching band is used to explain the role of hydrogen bonding behind the change of  $T_g$ . **Figure S5** illustrated FTIR spectrum of one of

CNW/TPUs—TPUC20 and the pure elastomer—TPU after water immersion for different time (~712 hour). From **Figure S5** (a) and (b), the band for free C=O ( $1704\text{ cm}^{-1}$ ) does not change during the whole immersion, whereas the hydrogen bonded C=O ( $1730\text{-}1731\text{ cm}^{-1}$ ) starts the downward shift after long time immersion. For TPUC20, after immersion for 262 hour, the peak shift from  $1731$  to  $1729\text{ cm}^{-1}$  can be observed. And in TPU, the obvious peak shift appears after immersion for dozens of hours. The trend is summarized in **Figure S5** (c). The aggrandizement of hydrogen bonds between absorbed water molecules and carbonyl group is the main reason. It leads to the band shift of free C=O to low frequency side. In nature, such a trend is similar to the shift of free C=O stretching to hydrogen bonded C=O stretching in the reported SMPs<sup>6</sup>. In the reported commercial SMPs, the water absorption process is much dependant on immersion time and hydrophilicity of SMPs. In that, the reported water driven shape recovery takes hours (432 hours) at ambient temperature to absorb up to 4.6% of weight fraction of moisture, because the extent of  $T_g$  decrease mostly relies on the amount of absorbed water (bonded water)<sup>7</sup>. Instead, in CNW/TPUs, it can be inferred that the water molecules firstly penetrate and induce the decoupling of the interaction among whiskers, which results in the disruption of whisker percolation network. The large amount of water is not needed for such a procedure according to the water immersion test shown in **Figure S6**. The rapid disruption of whisker percolation is achieved and evidenced by DMA results illustrated in **Figure 4**. In this stage, the weight ratio of absorbed water in CNW/TPUs is very low (<0.5 wt% after immersion in water for 10 mins), and easily and rapidly achieved at ambient condition.

Keeping immersing in water for hours (420.3 hours) make more water penetrate into elastomer matrix and form more hydrogen bonds with polymer chain, until the equilibrium weight ratio is reached after hundreds of immersion hours.

### S6. Weight ratio of absorbed water during immersion in water

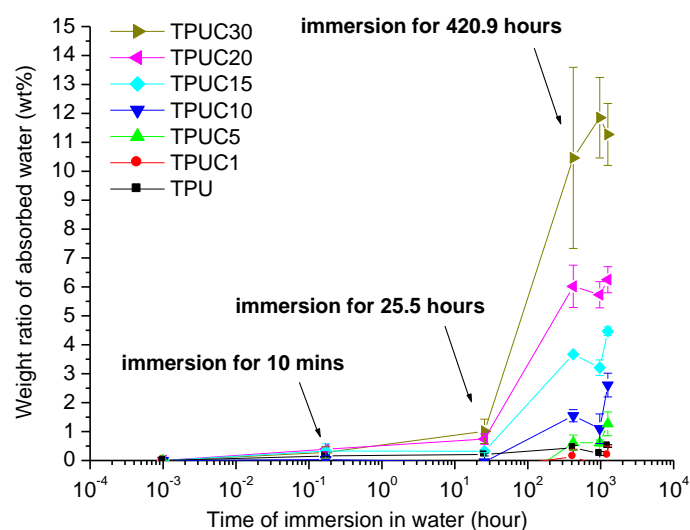


**Figure S6.** Weight ratio of absorbed water in CNW/TPUs during immersion in water. Dots represent the average values (number of individual measurement is 3)  $\pm$  standard deviation.

### S7. Polarized Raman spectra

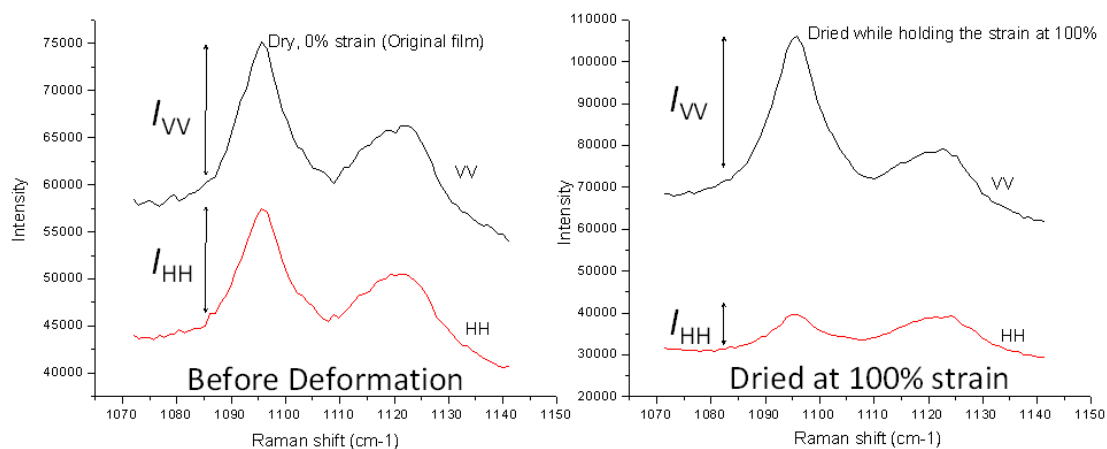


**Figure S7.** Polarized Raman spectra of the sample TPUC30 before deformation and after drying in deformed status respectively

## References

- [1] V. Favier, G.R. Canova, S.C. Shrivastava, J.Y. Cavaille, *Polym. Eng. Sci.* **1997**, 37 1732-1739.
- [2] V. Favier, R. Dendievel, G. Canova, J.Y. Cavaille, P. Gilormini, *Acta Mater.* **1997**, 45 1557-1565.
- [3] P. Hajji, J.Y. Cavaille, V. Favier, C. Gauthier, G. Vigier, *Polym. Compos.* **1996**, 17 612-619.
- [4] K. Shanmuganathan, J.R. Capadona, S.J. Rowan, C. Weder, *J. Mater. Chem.* **2010**, 20 180-186.
- [5] J.R. Capadona, K. Shanmuganathan, D.J. Tyler, S.J. Rowan, C. Weder, *Science* **2008**, 319 1370-1374.
- [6] B. Yang, W.M. Huang, C. Li, L. Li, *Polymer* **2006**, 47 1348-1356.
- [7] B. Yang, W.M. Huang, C. Li, C.M. Lee, L. Li, *Smart Mater. Struct.* **2004**, 13 191-195.